SUPPORTING INFORMATION

Dual Targeted Delivery of Liposomal Hybrid Gold Nano-assembly for Enhanced Photothermal Therapy Against Lung Carcinomas

Unnati Patel,* Kavini Rathnayake, Nirupama Singh, Emily C. Hunt

Department of Chemistry, The University of Alabama in Huntsville, Huntsville, AL 35899

Corresponding author.

Tel.: +1-2055677409

E-mail address: up0004@uah.edu

1. Additional Experimental Section

Materials and instruments. Hexadecyltrimethylammonium bromide (CTAB, 99%), L-ascorbic acid (AA, 98%), silver nitrate ($AgNO_3$, 99%), hydrogen tetrachloroauric (III) acid trihydrate ($HAuCl_4 \cdot 3H_2O$, 99.9%), sodium borohydride ($NaBH_4$, 98%), tetraethyl orthosilicate (TEOS, 98%), 3-aminopropyl-triethoxysilane (APTES, 97%), 3-(aminopropyl)trimethoxysilane (APTMS) (97%), *N*-hydroxysulfosuccinimide sodium salt (sulfo-NHS), rhodamine B isothiocyanate isomer (RITC), 4',6'-diamidino-2-phenylindole (DAPI, 98%), folic acid, doxorubicin, chlorpromazine nystatin, and wortmannin were purchased from Sigma-Aldrich (St. Louis, USA). Sodium hydroxide (NaOH, 98.5%) was purchased from Lab Chem (Pennsylvania, USA). Ammonium nitrate (NH_4NO_3, 99%) was purchased from ACROS Organics. 1-ethyl-3-(3-dimethylaminopropyl)- carbodiimide (EDC, 98%) was purchased from Alfa Aesar (Massachusetts, USA) and *N*-hydroxysuccinimide (NHS, 99%), was purchased from TCI America (Portland, USA). Water was used from a Milli-Q water ultrapure water purification system (Millipore). Absolute ethanol (200 proof) was purchased from Fisher Scientific Inc., (Massachusetts, USA). 1,2-dipalmitoyl-*sn*-glycero-3-phosphocholine (DPPC), cholesterol and 1,2-distearoyl-*sn*-glycero-3-phosphoethanolamine-*N*-[amino(polyethylene glycol)-2000] (DSPE-PEG 2000 amine), and a mini extruder kit were purchased from Avanti Polar Lipids Inc. (Alabama, USA). GE11 peptide (Tyr-His-Trp-Tyr-Gly-Tyr-Thr-Pro-Gln-Asn-Val-Ile) was obtained from Phoenix Pharmaceuticals, Inc (California, USA). A549 lung cancer cells (ATCC, CCL-185) and MRC-5 healthy lung cell line (ATCC, CCL-171) were purchased from American Type Culture Collection (Virginia, USA). The CellEvent™ Caspase 3/7 Green Detection Reagent, Live/dead® viability kit, MitoProbe™ JC-1 assay kit, Tubulin Tracker™ Green Detection kit, and Scientific and

Invitrogen™ ATP Determination kit was purchased from ThermoFisher Scientific (New Jersey, USA). Fluorometric intercellular ROS kit and MES buffer were purchased from Sigma-Aldrich (St. Louis, USA). The GSH-Glo™ Glutathione assay was purchased from Promega Corporation (Wisconsin, USA). (3- (4,5-Dimethylthiazol-2-yl)-2,5-diphenyltetrazolium bromide) (MTT) cell proliferation kit, 4′,6-diamidino-2-phenylindole (DAPI), and calcein AM were purchased from ThermoFisher Scientific (Massachusetts, USA). Ham's F- 12K nutrient mixture with L-glutamine (F-12K, 1X), fetal bovine serum (FBS, 10%), trypsin EDTA (2.21 mM), and penicillin streptomycin (Pen-Strep, 1X) were obtained from Corning (New York, USA).

The particle size was determined by using transmission electron microscopy (TEM). TEM images were obtained on a FEI Tecnai Osiris operating at an accelerating voltage of 200 kV. Nitrogen adsorption-desorption was performed using a surface area and porosity analyzer (Autosorb iQ-C-MP/XR, USA). Absorbance spectra of particles and optical density measurements were performed with a Spectramax M2 Molecular Devices Ltd., plate reader (Silicon Valley, USA). Fourier-Transform Infrared (FTIR) spectroscopic analysis was done using Nicolet is50 ATR FTIR ThermoFisher Scientific (New Jersey, USA). Thermogravimetric analysis (TGA) was performed on a Discovery Q500 TGA from TA Instruments (Massachusetts, USA). The 808 nm laser diodes (G pin code) of 200 mW and 500 mW power intensities, laser diode controller (LDC210C), laser diode temperature controller (TED200C), laser diode mount (LDM56), digital thermometer, and 25 mm objective lens (LA1560) were all purchased from Thor Labs Inc., (New Jersey, USA). The fluorescence microscopy images were taken on a CKX53 inverted fluorescence microscope from Olympus (USA). The sterile mammalian cell cultures were conducted in separate 1300 Series A2 bio safety cabinet (ThermoFisher Scientific). Shaking incubator (Corning, USA) and CO_2 incubator (ThermoFisher Scientific) were used for mammalian cell culture incubation. Sterile

disposables, sterilized glassware, and medium were used for all experiments. Unless specifically mentioned, all liquid media were sterilized using a bench top BioClave liquid sterilizer (Ward's Science, New York, USA). Mammalian cells were quantified using CytoSMART automated cell counter (Corning, USA).

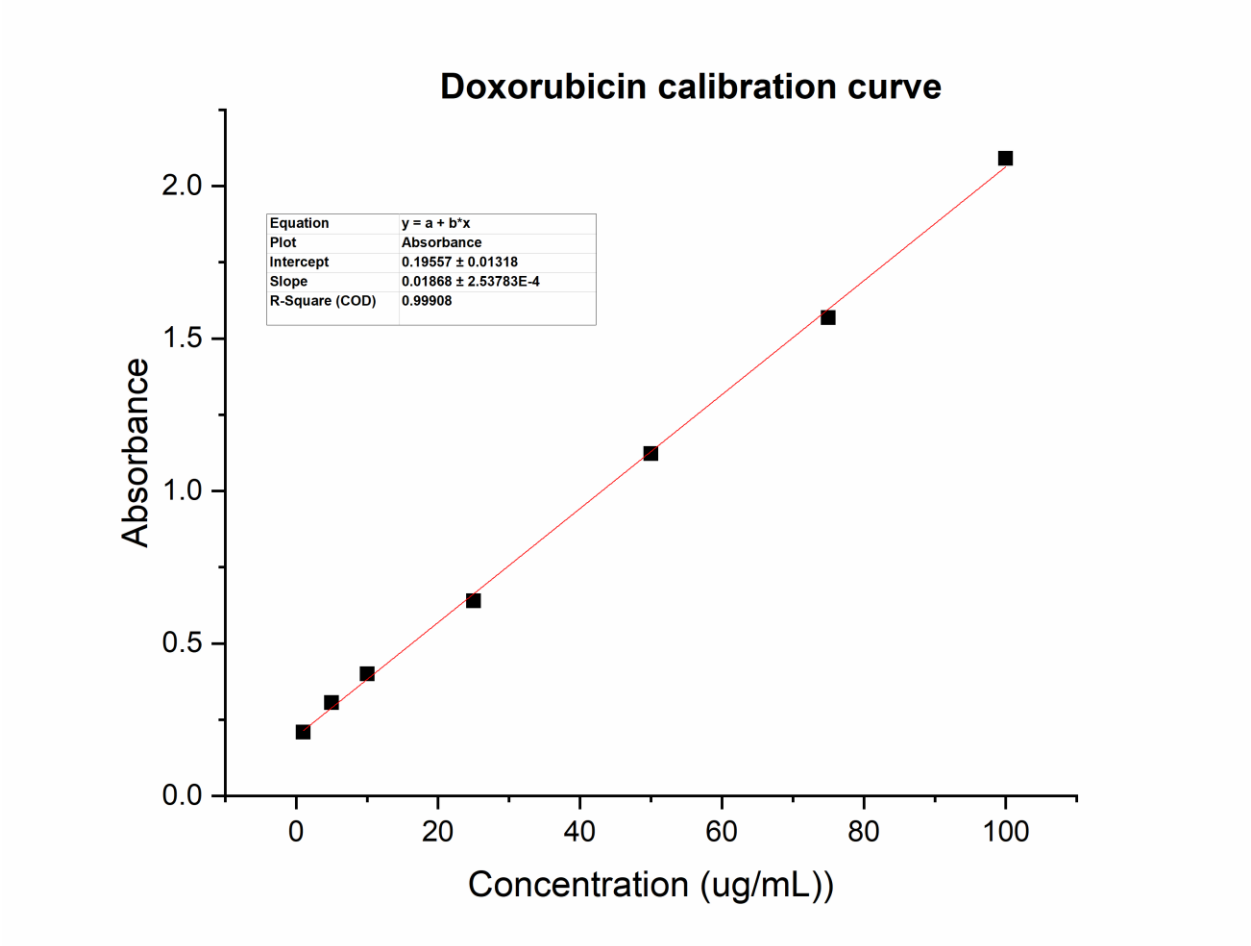

Figure S1. Standard calibration curve of Doxorubicin.

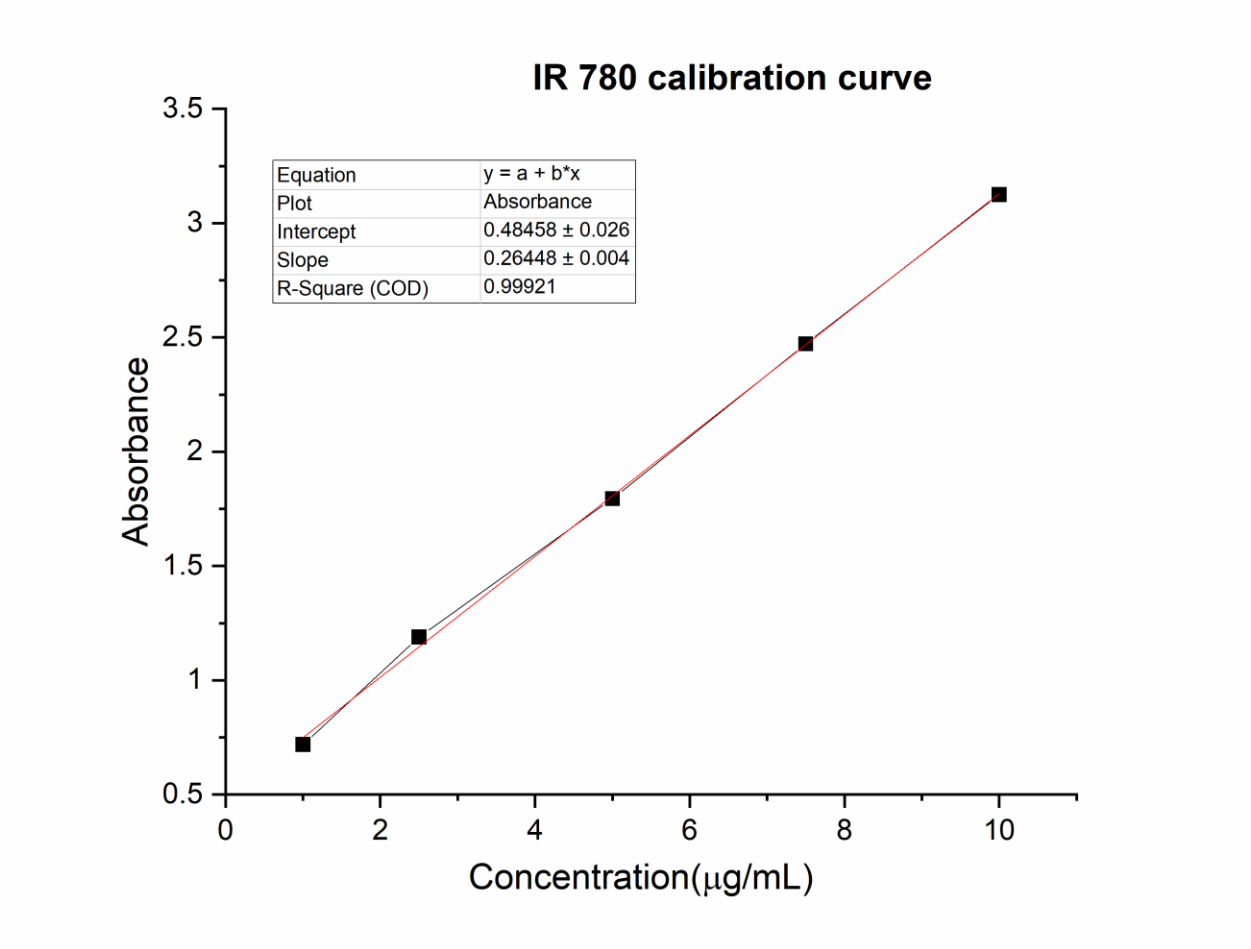

Figure S2. Standard calibration curve of IR 780.

To calculate % IR 780 in [(GM@Dox)LI]-PF using plate reader, the standard calibration series 1, 2.5, 5, 7.5 and 10 μg/mL of IR 780 at 780 nm was run as shown in Figure S2. The absorbance of the test samples [(GM@Dox)LI]-PF, [(GM@Dox)LI]-P, [(GM@Dox)LI]-F, [(GM@Dox)LI], [(GM@Dox)L, (GM@Dox) was also recorded. The absorbance of [(GM@Dox)LI]-PF was recorded at 780 nm. To avoid the influence of other components, we have excluded the absorbance of [(GM@Dox)LI]-P, [(GM@Dox)LI]-F, [(GM@Dox)LI] [(GM@Dox)L], (GM@Dox), from the absorbance of [(GM@Dox)LI]-PF and then calculated the amount of IR 780 using standard calibration curve (y= mx+c) equation.

$$y = mx + c \text{ equation,}$$

where, y = absorbance (at 780 nm from nano-assembly)
m = slope
b = intercept
x = amount of IR 780 presents on nano-assembly

To calculate the amount of GE-11 and folic acid, we did similar calculations using standard calibration of each.

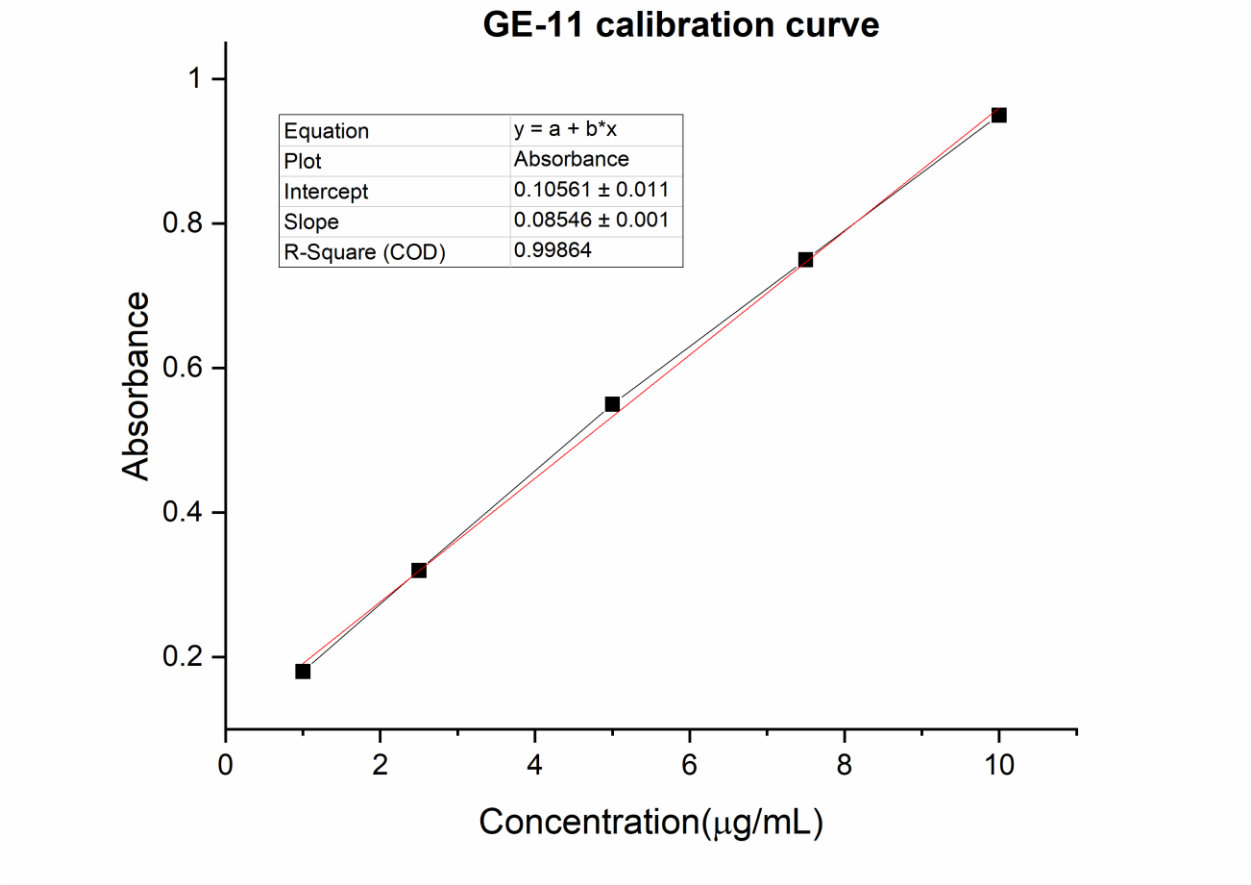

Figure S3. Standard calibration curve of GE-11 peptide.

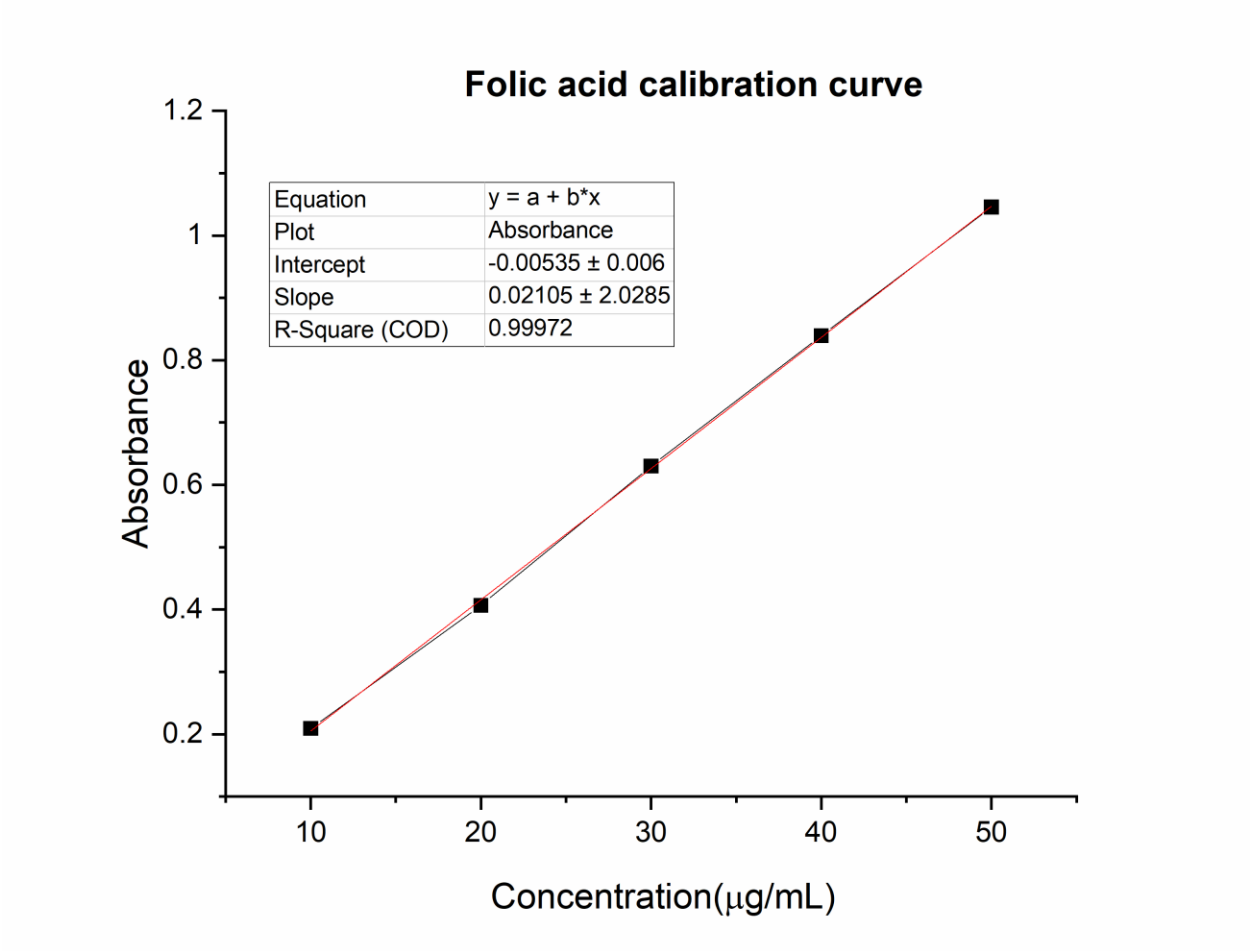

Figure S4. Standard calibration curve of folic acid.

Table S1. BET analysis of nano-assemblies

	GM	**GM@Dox**
Surface area (Multipoint BET)	53.852 m^2/g	42.060 m^2/g
Pore volume (BJH method)	0.23 cc/g	0.171 cc/g
Pore size (BJH method)	19.13 Å	12.19 Å

FT-IR analysis of various nano-assemblies: The FT-IR spectra of the various nano-assemblies obtained after each fabrication step are presented in Figure S5. As shown in Figure S5a, GNRs show -CH_2 symmetric and asymmetric vibrations at 2847 cm^{-1} and 2870 cm^{-1}, respectively. The presence of a peak at 1473 cm^{-1} corresponds to the -CH_2 scissoring mode of vibration. In the fingerprint region, the bands at 960 and 817 cm^{-1} are consistent with C-O stretching and in-plane C-H bending vibrations. The appearance of a peak at 1064 cm^{-1} (Si-O-Si stretching) and the disappearance of symmetric (2847 cm^{-1}) and asymmetric (2870 cm^{-1}) vibrations, which were seen in GNR, proves the mesoporous silica coating is on the surface of GNRs. The spectrum of free Dox showed characteristic peaks at 3311 cm^{-1} (OH and NH, stretch), 2,898 cm^{-1}(CH stretch, aromatic), 1,730 cm^{-1}(C=O stretch, ketone), 1,615 cm^{-1}(C=O stretch), 1,282 cm^{-1} (C-O-C, stretch), 1,115 cm^{-1}(C-O stretch, tertiary alcohol), 1,070 cm^{-1}(C-O stretch, secondary alcohol), and 988 cm^{-1}(C-O stretch, primary alcohol).[1] Similar trends in characteristic peaks were seen after loading Dox into GM, which confirms the successful loading of Dox.

Next, as shown in Figure S5b, the IR 780 loading inside the liposome and the liposome wrapping on GM@Dox were analyzed by comparing FTIR spectra of GM@Dox, [(GM@Dox) L], [(GM@Dox) LI], and IR 780. The symmetric and anti-symmetric -CH_2 stretching at 2850 cm^{-1} and 2920 cm^{-1} were the characteristic lines for the long carbon chain of the lipids used. Also, the C=O stretching vibration around 1737 cm^{-1} and the PO_2 symmetric stretching vibration around 1111 cm^{-1} are from phospholipids, confirming the successful liposome coating. IR 780 loading inside TSL was proved by comparing FTIR spectra of IR 780 and [(GM@Dox) LI]. As shown in Figure S5b, the trend of characteristic peaks of [(GM@Dox) LI], was similar to free IR 780, which confirms the loading of IR 780 dye inside the liposome.

Furthermore, the FTIR spectra of [(GM@Dox) LI]-PF and free GE-11 were recorded to verify that the GE11 peptide had been conjugated to [(GM@Dox) LI]. The intense broad band at 3289 cm^{-1} in Figure S5c represents N-H stretching vibrations, indicating the presence of amino groups. We assign two sharp absorption bands at 1647 and 1515 cm^{-1} to the amide I and amide II groups of the GE11 peptide, respectively.[2] By contrast, the absorption bands for the amide I and amide II groups of the[(GM@Dox) LI]-PF nano-assemblies appeared at 1637 and 1553 cm^{-1}, respectively (Figure 3b). The shifts of these two amide absorption bands to the higher wavenumber suggest that conformational changes occurred to the GE11 peptide upon binding to [(GM@Dox) LI]. The presence of C=O groups in free GE11 peptide at 1444 cm^{-1} correspond to the symmetrical stretching vibrations of carboxylate groups, while in [(GM@Dox) LI]-PF nano-assemblies, this shift to a higher wavenumber 1517 cm^{-1} suggests that conformational change occurred to the GE11 peptide upon binding to [(GM@Dox) LI].

The conjugation of folic acid on to [(GM@Dox) LI] was investigated by comparing free folic acid and [(GM@Dox) LI]-PF. The characteristic IR absorption peaks at 1690 and 1601 cm^{-1} are observed in the spectrum of free folic acid, due to C=O amide stretching of the α-carboxyl group and absorption of aromatic C=C group respectively.[3-4] While the absorption bands of the [(GM@Dox) LI]-PF nano-assemblies appeared at 1732 and 1636 cm^{-1}, respectively. Again, the wavenumber shifting to higher range indicated that conformational changes occurred to the folic acid upon conjugation with [(GM@Dox) LI]. From all these FTIR spectra, we have successfully confirmed the fabrication of the nano-assemblies after each step of synthesis.

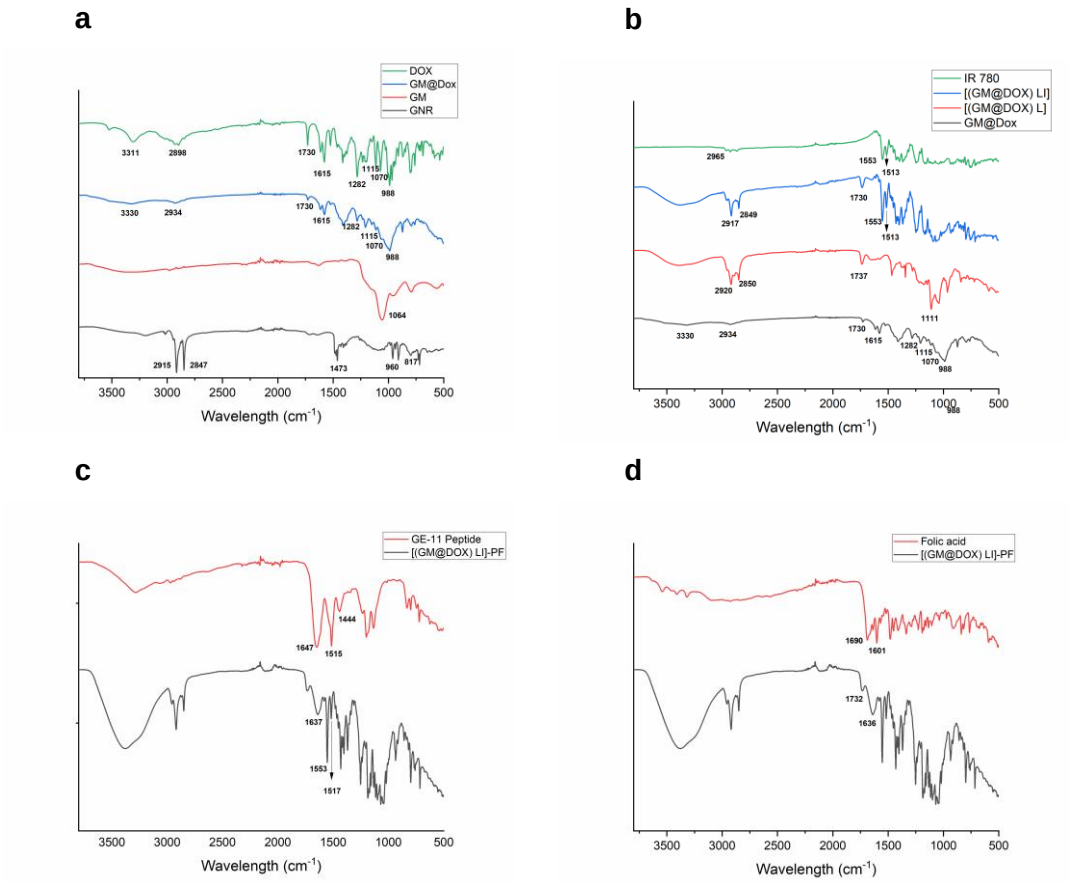

Figure S5. FTIR analysis of various nano-assemblies synthesized after each step. (a) Comparison of between GNR, GM, GM@Dox, and free Dox. (b) FTIR spectra of GM@Dox, [(GM@Dox) L], [(GM@Dox) LI], and free IR 780. Comparative FTIR spectrum of free (c) GE-11 with [(GM@Dox) LI]-PF and (d) FA with [(GM@Dox) LI]-PF.

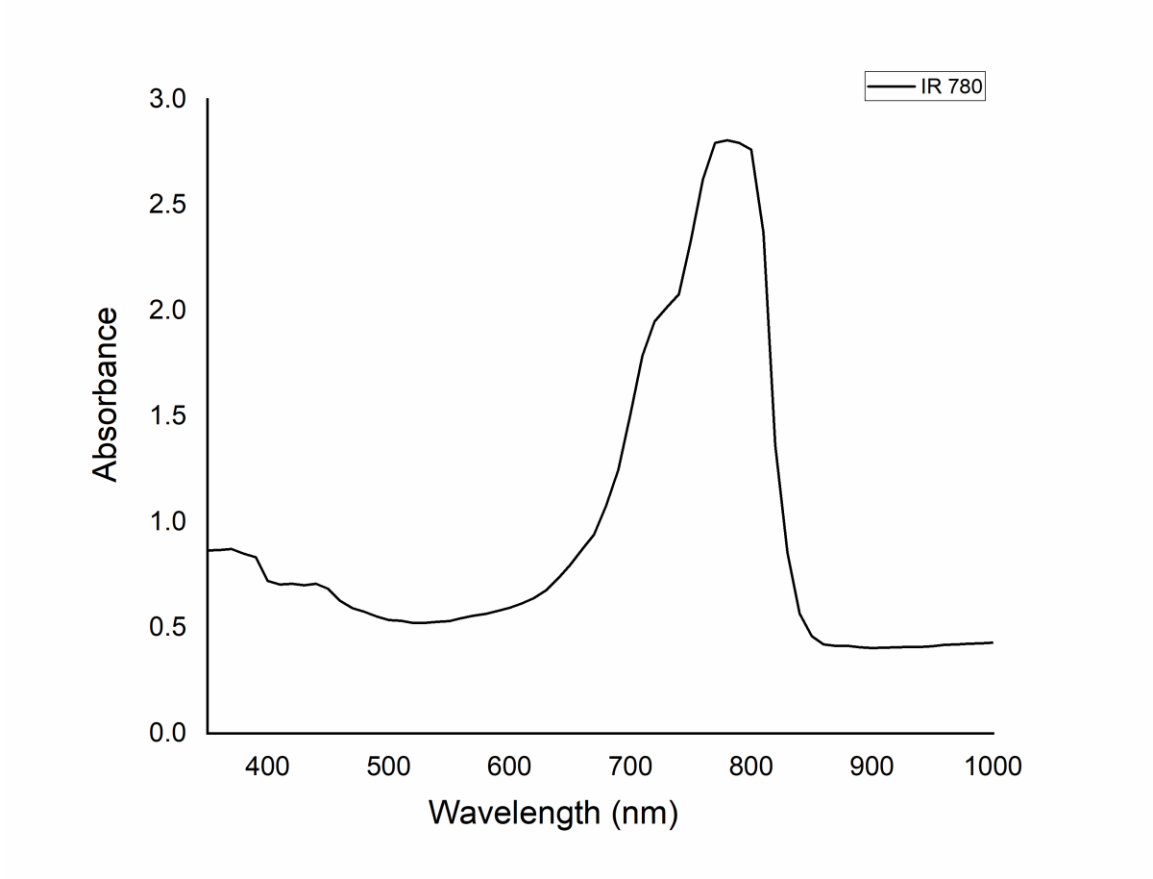

Figure S6. UV-vis spectrum of bare IR 780.

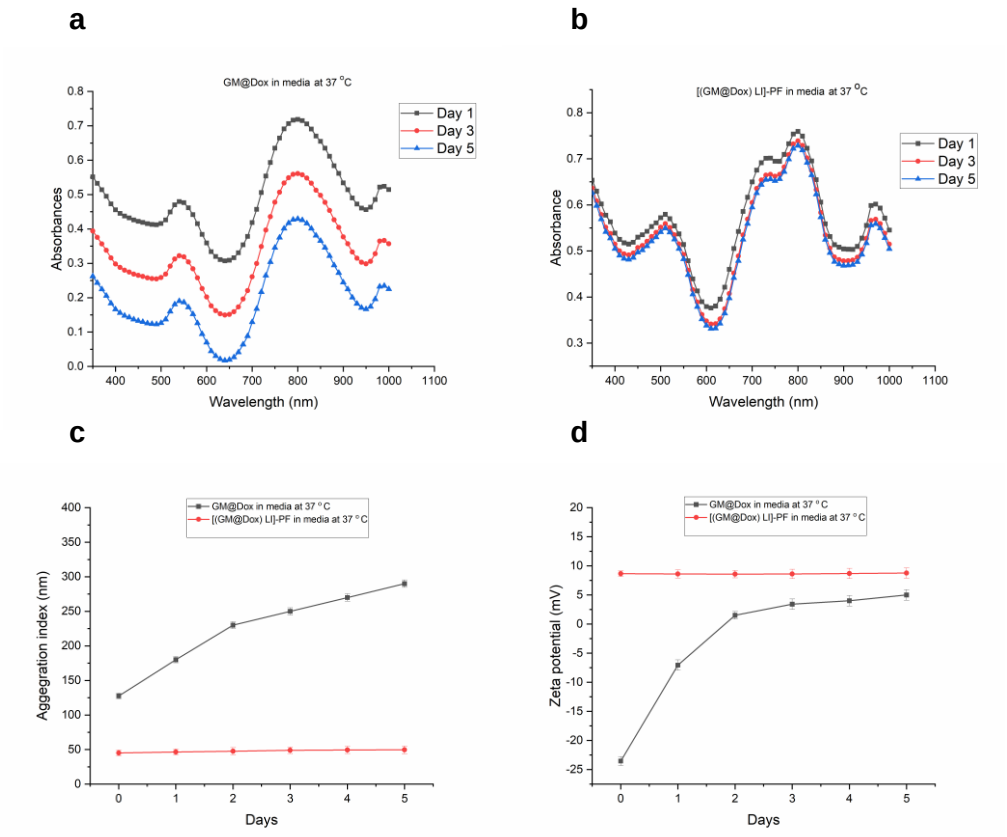

Figure S7. Colloidal stability analysis of GM@Dox and[(GM@Dox) LI]-PF. UV-vis spectra of (A) GM@Dox (B) [(GM@Dox) LI]-PF at 37 °C, in cell culture media. (C) Aggregation index (AI) of GM@Dox and[(GM@Dox) LI]-PF. (D) Zeta potential of GM@Dox and[(GM@Dox) LI]-PF in cell culture media at 37 ◦C.

Colloidal stability: We next investigated the colloidal stability of GM@Dox and [(GM@Dox) LI]-PF during storage. As depicted in Figure S7, the LSPR peak intensity, aggregation index, and zeta potential of [(GM@Dox) LI]-PF were stable during storage for 5 days, reflecting the excellent stability of the prepared [(GM@Dox) LI]-PF due to the presence of the liposomal layer, while GM@Dox was not stable for 5 days as shown by the reducing LSPR peak intensity and the altering aggregation index and zeta potential.

Assessment of Targeting affinity of [(GM@Dox) LI]-PF towards MRC-5 (healthy lung cell line)

In this experiment, we have treated MRC-5 cell line (healthy lung cell lines) with [(GM@Dox) LI]-PF in presence of laser then incubated for 6 h. As shown in Figure S8, [(GM@Dox) LI]-PF treated healthy cells not showing red fluorescent (coming from Dox) which proves that [(GM@Dox) LI]-PF nano-assembly specifically target the cancerous A549 cells without affecting the healthy cells.

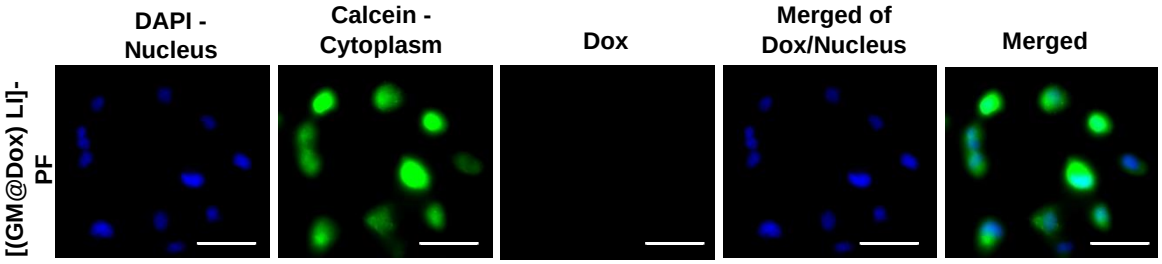

Figure S8. Targeting affinity of MRC-5 healthy cells treated with [(GM@Dox) LI]-PF in presence of laser. The nano-assembly has Dox which has red fluoroscence and the A549 cells and the nuclei were stained with Calcein AM and DAPI respectively. (Scale bar, 10 μm).

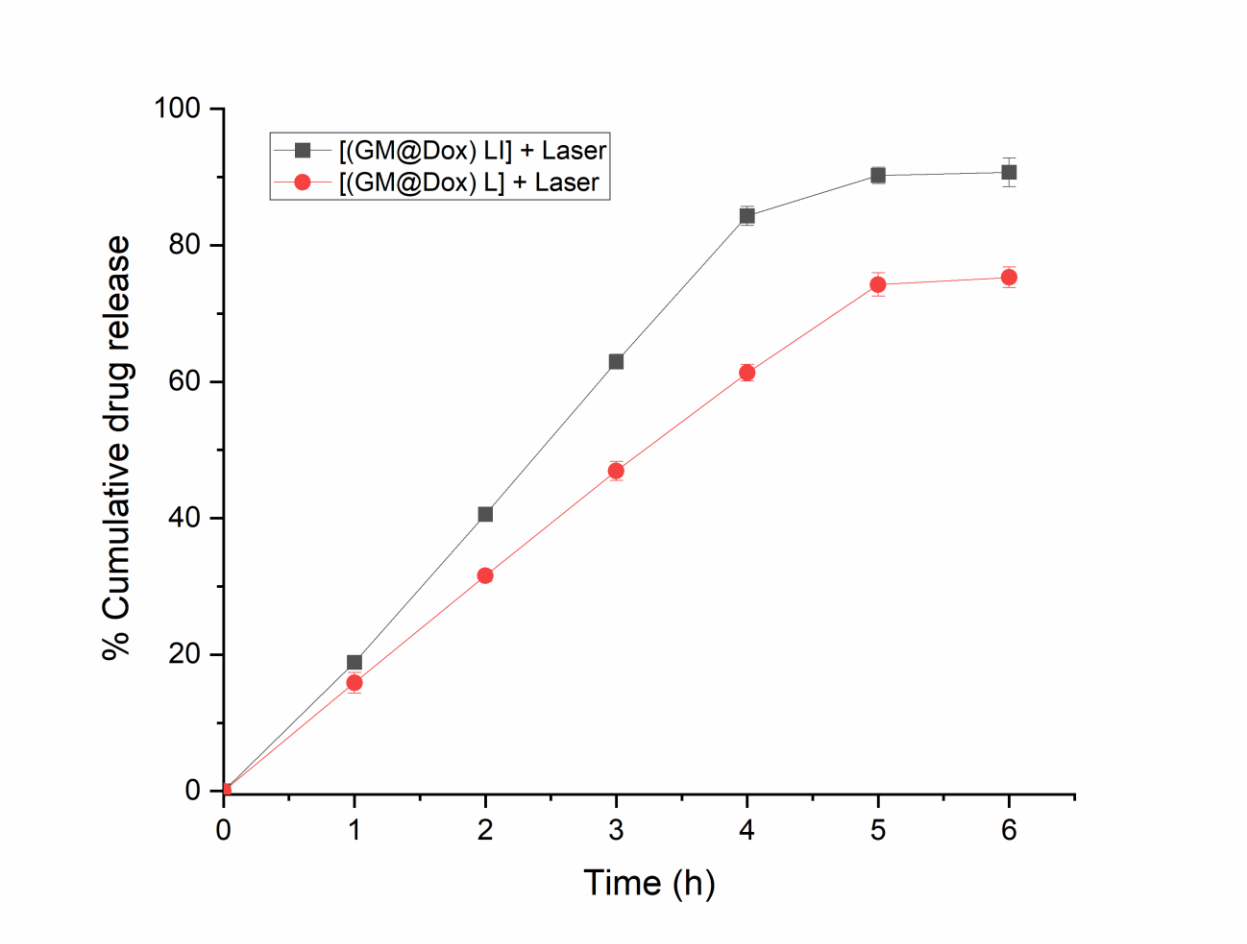

Figure S9. Cumulative drug release profile of Dox for [(GM@Dox) L] and [(GM@Dox) LI] nano-assemblies with laser irradiation (808 nm, 350 mW, 15 min).

Cell uptake mechanism: The primary mechanism by which nanoparticles are transported into cells is endocytosis. At least four fundamental pathways are involved in endocytosis: caveolae-mediated endocytosis, clathrin-mediated endocytosis, macropinocytosis, and clathrin- and caveolae-independent endocytosis.[5] Clathrin-mediated endocytosis is well-known for its function in the selective ingestion of molecules via unique receptors by all eukaryotic cells to internalize nutrients and degrade or recycle substances.[6-7] Specific endocytosis inhibitors: chlorpromazine (an inhibitor of clathrin-mediated endocytosis), nystatin (an inhibitor for caveolin- dependent endocytosis), and wortmannin (a macropinocytosis inhibitor) were investigated to study the mechanism of cellular uptake.[8] The mechanism for the internalization of the nano-assemblies into the lung cells was monitored by fluorescence microscopy (Figure S10a). The cellular uptake mechanism of RITC - GM@Dox and RITC – [(GM@Dox) LI]-PF in A549 cells was determined under different endocytosis-inhibited conditions. We have also quantified the cellular uptake of nano-assemblies using fluorescent assays. The fluorescence microscopy images reveal little or no visible red fluorescent RITC – [(GM@Dox) LI]-PF in chlorpromazine treated A549 cells (Figure S10b), which indicates chlorpromazine treated lung cells shows inhibited uptake of RITC – [(GM@Dox) LI]-PF. However, uptake of RITC – [(GM@Dox) LI]-PF into lung cells was not hindered when treated with wortmannin and nystatin (Figure S10 and Figure S10b). These observations suggested that the trafficking of the nano-assemblies occurred preferably through a clathrin-mediated endocytosis.

To investigate the role of the liposome in cellular uptake, we quantified the cellular uptake of RITC-labelled nano-assemblies GM@Dox and [(GM@Dox) LI]-PF by measuring the intracellular fluorescence intensity using a fluorescence microplate reader. Liposome coating is known to enhance the cellular uptake of nano-assemblies due to interaction with the lipophilic cell membrane that allows cellular entry of nanoparticles by various endocytosis pathways.[8] In addition, the liposome was modified with the cationic peptide GE-11, so due to electrostatic interactions with negatively charged cell membrane, the cellular uptake was higher for [(GM@Dox) LI]-PF as compared to GM@Dox. As shown in Figure S10b, chlorpromazine, an inhibitor of clathrin-mediated endocytosis, significantly inhibited both GM@Dox and [(GM@Dox) LI]-PF delivery into A549 cells. The quantified intracellular uptake of GM@Dox and [(GM@Dox) LI]-PF was 8.1 ± 1.2 % and 27.01 ± 1.5 % respectively. Even in the presence of the inhibitor, a higher amount of [(GM@Dox) LI]-PF uptake was found in A549 cells, which

indicates that the inclusion of the liposome and the cationic peptide (GE-11) increases the ability of the cells to internalize the nano-assembly. Throughout all inhibitory assays, GM@Dox has consistently shown a lesser amount of uptake (Figure S10b). These studies collectively suggested that the nano-assembly-mediated drug delivery occurred preferably through clathrin-mediated endocytosis, and nano-assembly internalization was enhanced due to the presence of the liposome and GE-11 cationic peptide.

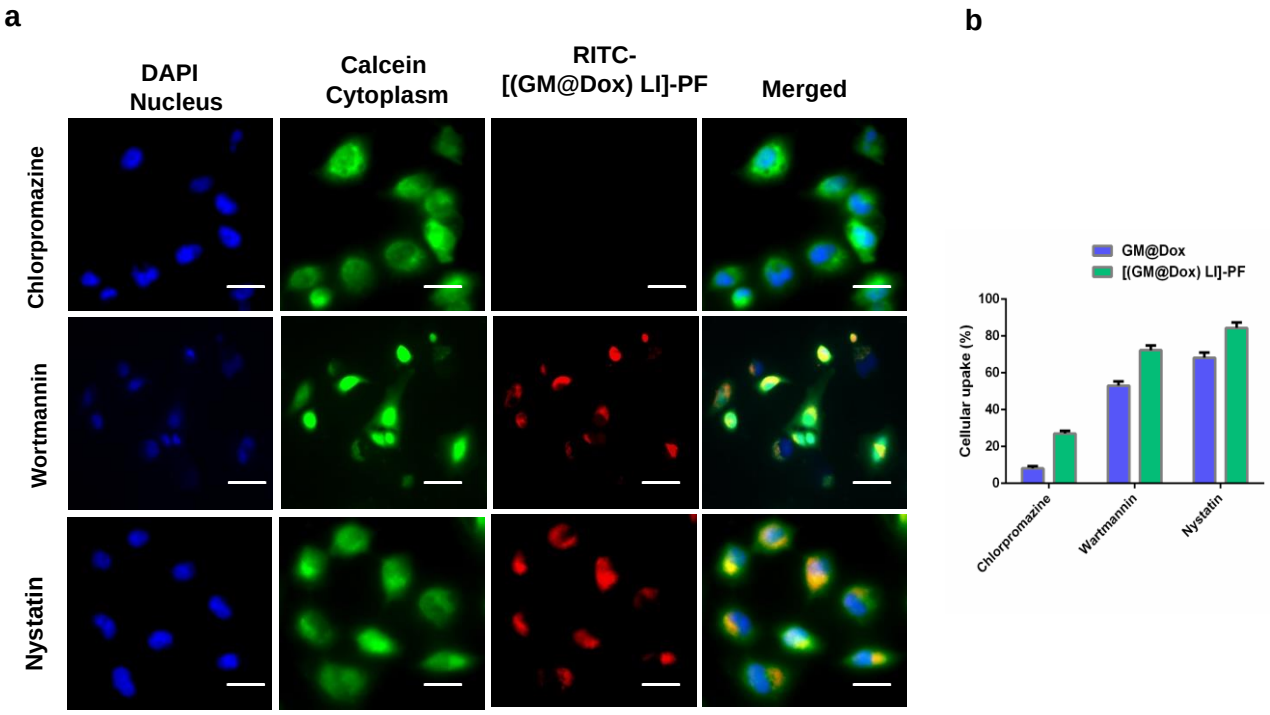

Figure S10. (a) Evaluation of cell uptake mechanism of nano-assemblies by A549 cells under different endocytosis inhibitory conditions - fluorescence microscopy – A549 cells are stained with calcein dye (green), cell nucleus stained with DAPI (blue), [(GM@Dox) LI]-PF were labelled with red fluorescent RITC dye (red). Scale bar: 10 μm. (b) Shows quantitative intracellular uptake of GNR@MSNP@BDQ and GNR@MSNP@BDQ@TSL@NZX by A549 cells after inhibitor treatment.

Assessment of MRC-5 cell viability after treatment with [(GM@Dox)LI]-PF by MTT assay:

The cell viability assay on MRC-5 healthy lung cell lines was conducted using MTT assay. MRC-5 cells were treated with 50 μg/mL of [(GM@Dox)LI]-PF. After 3 h of incubation, the cells were irradiated with 808nm laser (350 mW) for 15 min and further incubated for 3 h. A 100 μL aliquot of MTT (5 mg/mL) was added to each well, and the plate was further incubated for 3 h. The culture medium in each well was replaced with 100 μL of DMSO and the plate was gently agitated for 10 min. Similarly, cells were treated without NIR laser after incubating with nano-assemblies. To check the effect of alone laser on healthy cells, we have treated MRC-5 cells with and without laser and followed similar procedure as explained above. The percentage viability was calculated by comparing untreated cells to treated cells, and the absorbance was measured at 590 nm using a plate reader.

We have observed almost little to no toxicity effect of laser on MRC-5 cells. When the cells were treated with [(GM@Dox)LI]-PF in the presence and absence of laser, there was no toxic effect on MRC-5 cells, indicating that the cell viability is nearly 100%. This observation indicates that [(GM@Dox)LI]-PF nano-assembly is not toxic to healthy cells.

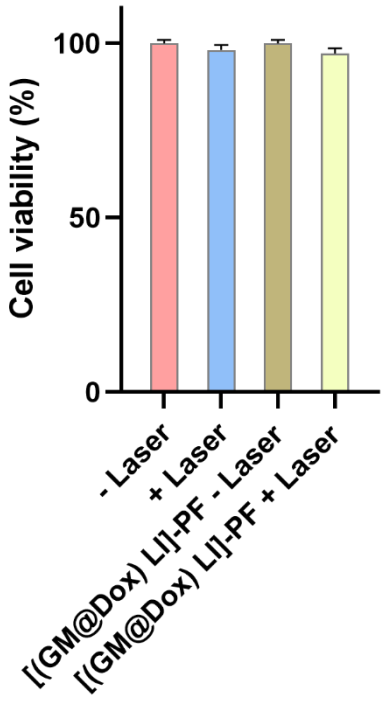

Figure S11. Assessment of healthy lung cells viability after treatment with laser and [(GM@Dox)LI]-PF by MTT assay.

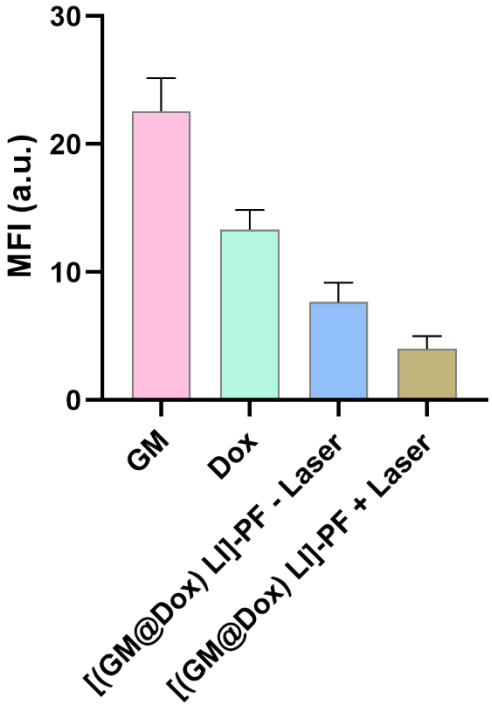

Figure S12. Quantitative analysis of green fluorescence density of cytoplasm of A549 cells, treated with nanomaterials. Each analysis was recorded on at least 25 cells using Fiji software. The Data was presented as the mean ± SD (n=3).

REFERENCES

(1) Kanwal, U.; Bukhari, N. I.; Rana, N. F.; Rehman, M.; Hussain, K.; Abbas, N.; Mehmood, A.; Raza, A. Doxorubicin-loaded quaternary ammonium palmitoyl glycol chitosan polymeric nanoformulation: uptake by cells and organs. *International journal of nanomedicine* **2018,** *14*, 1-15.
(2) Pi, J.; Jiang, J.; Cai, H.; Yang, F.; Jin, H.; Yang, P.; Cai, J.; Chen, Z. W. GE11 peptide conjugated selenium nanoparticles for EGFR targeted oridonin delivery to achieve enhanced anticancer efficacy by inhibiting EGFR-mediated PI3K/AKT and Ras/Raf/MEK/ERK pathways. *Drug Delivery* **2017,** *24* (1), 1549-1564.
(3) Zhang, Y.; Kohler, N.; Zhang, M. Surface modification of superparamagnetic magnetite nanoparticles and their intracellular uptake. *Biomaterials* **2002,** *23* (7), 1553-1561.
(4) Rana, S.; Shetake, N. G.; Barick, K. C.; Pandey, B. N.; Salunke, H. G.; Hassan, P. A. Folic acid conjugated Fe3O4 magnetic nanoparticles for targeted delivery of doxorubicin. *Dalton Transactions* **2016,** *45* (43), 17401-17408.
(5) Liu, J.; Shapiro, J. I. Endocytosis and signal transduction: basic science update. *Biological research for nursing* **2003,** *5* (2), 117-128.
(6) Mahmoudi, M.; Azadmanesh, K.; Shokrgozar, M. A.; Journeay, W. S.; Laurent, S. Effect of nanoparticles on the cell life cycle. *Chemical reviews* **2011,** *111* (5), 3407-3432.
(7) Gao, H.; Yang, Z.; Zhang, S.; Cao, S.; Shen, S.; Pang, Z.; Jiang, X. Ligand modified nanoparticles increases cell uptake, alters endocytosis and elevates glioma distribution and internalization. *Scientific reports* **2013,** *3* (1), 1-9.
(8) Behzadi, S.; Serpooshan, V.; Tao, W.; Hamaly, M. A.; Alkawareek, M. Y.; Dreaden, E. C.; Brown, D.; Alkilany, A. M.; Farokhzad, O. C.; Mahmoudi, M. Cellular uptake of nanoparticles: journey inside the cell. *Chemical Society Reviews* **2017,** *46* (14), 4218-4244.